Article

Reactant Concentrations from Fluorescence Correlation Spectroscopy with Tailored Fluorescent Probes. An Example of Local Calibration-Free pH Measurement

Sandrine Charier, Adrien Meglio, Damien Alcor, Emmanuelle Cogn-Laage, Jean-Franois Allemand, Ludovic Jullien, and Annie Lemarchand

J. Am. Chem. Soc., **2005**, 127 (44), 15491-15505• DOI: 10.1021/ja053909w • Publication Date (Web): 18 October 2005

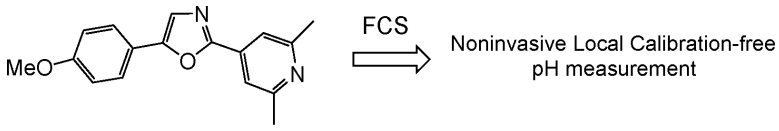

More About This Article

Additional resources and features associated with this article are available within the HTML version:

- Supporting Information
- Links to the 3 articles that cite this article, as of the time of this article download
- Access to high resolution figures
- Links to articles and content related to this article
- Copyright permission to reproduce figures and/or text from this article

View the Full Text HTML

J|A|C|S
ARTICLES
Published on Web 10/18/2005

Reactant Concentrations from Fluorescence Correlation Spectroscopy with Tailored Fluorescent Probes. An Example of Local Calibration-Free pH Measurement

Sandrine Charier,[†] Adrien Meglio,[†] Damien Alcor,[†] Emmanuelle Cogné-Laage,[†] Jean-François Allemand,[†,‡] Ludovic Jullien,*[,†] and Annie Lemarchand[§]

Contribution from the Département de Chimie (CNRS UMR 8640), École Normale Supérieure, 24, rue Lhomond, 75231 Paris Cedex 05, France, the Département de Physique (CNRS UMR 8550), École Normale Supérieure, 24, rue Lhomond, 75231 Paris Cedex 05, France, and the Laboratoire de Physique Théorique de la Matière Condensée (CNRS UMR 7600), Université Pierre et Marie Curie, 4, place Jussieu, 75252 Paris Cedex 05, France

Received June 14, 2005; E-mail: Ludovic.Jullien@ens.fr

Abstract: The present account is concerned with the measurement of local reactant concentrations by observing specific fluorescent probes in fluorescence correlation spectroscopy (FCS). The Theoretical Analysis section revisits the photophysical, thermodynamic, and kinetic information that is contained in the corresponding FCS correlation curves. In particular, we examine the conditions under which FCS is revealed as a superior tool to measure concentrations of reactive species. Careful molecular engineering of the specific fluorescent probes that simultaneously integrates photophysical, thermodynamic, and kinetic constraints will be required to benefit most from FCS. We illustrate the FCS titration approach with a series of fluorescent probes that we tailored to measure pH at around 4−6 by FCS after two-photon excitation. We show that an optimal design allows one to access pH without any preliminary calibrations such as the determination of the protonation constant or the photophysical properties of the fluorescent probe.

1. Introduction

There is a growing interest in the determination of the spatial and temporal distribution of individual components in chemical and biological systems. In principle, the concentration H in a component $\mathscr{H}$ can be deduced from measuring the local and instantaneous intensity of a signal that arises from its atoms or its characteristic groups (fluorescence emission is used here for illustration).[1−3] One can also use its reactivity and perform titrations with $\mathscr{H}$-specific reagents; this may overcome limitations intrinsic to the $\mathscr{H}$ structure. For instance, even when $\mathscr{H}$ is nonfluorescent such as in the present experimental system, $\mathscr{H}$ titration can rely on fluorescence emission if reaction 1 of

$$\mathscr{A}\mathscr{H} \rightleftharpoons \mathscr{A} + \mathscr{H} \qquad (1)$$

$\mathscr{H}$ with a fluorescent reagent $\mathscr{A}$ yields a product, $\mathscr{A}\mathscr{H}$, that exhibits a different brightness.

Using the latter strategy, a first approach to access H consists of converting, in concentration terms, the intensity of fluorescence emission that arises from the illuminated volume at a given wavelength. Then, to extract H requires knowledge of (i) the characteristics of the instrumental setup, (ii) the total concentration C in the fluorescent reagent, (iii) the properties of absorption and emission of $\mathscr{A}\mathscr{H}$ and $\mathscr{A}$, and (iv) the equilibrium constant of reaction 1.

On the basis of the ratio of the emission intensities at two different wavelengths, the more favorable ratiometric determination of H no longer requires the knowledge of (i) and (ii) but still requires that of (iii) and (iv).[2,3] A similar approach relies on a biexponential analysis of the decay of fluorescence emission; H is then determined after evaluation of the amplitude of the terms associated to $\mathscr{A}\mathscr{H}$ and $\mathscr{A}$, respectively.[4]

Data (i)−(iv) are generally derived from preliminary calibrations that are not always relevant to all the situations such as, for instance, those encountered in biology. Living cells are optically heterogeneous: the shape of the illuminated volume and the collection factor of the experimental setup are difficult to evaluate from calibrations. The concentration C often remains unknown in vivo. Eventually, the photophysical features of $\mathscr{A}\mathscr{H}$ and $\mathscr{A}$, as well as the thermodynamic properties of reaction 1, can be significantly altered in biological media. In fact, analyses yielding H with more "robust" prerequisites would represent attractive improvements.

* Fax: (+33) 1 44 32 33 25.
[†] Département de Chimie, École Normale Supérieure.
[‡] Département de Physique, École Normale Supérieure.
[§] Université Pierre et Marie Curie.

(1) Cantor, C. R.; Schimmel, P. R. *Biophysical Chemistry*; Part II; Freeman: New York, 1980.
(2) Lakowicz, J. R. *Principles of Fluorescence Spectroscopy*; Plenum Press: New York, 1999.
(3) Valeur, B. *Molecular Fluorescence Principles and Applications*: Wiley VCH: Weinheim, New York, Chichester, Brisbane, Singapore, Toronto, 2002.
(4) See, for instance: Draxler, S.; E.L., M.; Lippitsch, M.; Leiner, J.-P. *Sens. Actuators, B* **1993**, *11*, 421−424.

The analysis of density fluctuations in an open system at equilibrium provides a rich body of information related to concentrations. Thermodynamics is contained in the fluctuation amplitude, whereas kinetics lies in the time-dependent decay of the correlation of the fluctuations.[5−7] Techniques making use of fluctuation analysis are robust; they do not require any signal calibration, but only the knowledge of the system extent. Fluorescence correlation spectroscopy (FCS) is a technique relying on the preceding principle.[8−17] In relation to the titration issue, solution-based[18] FCS has been theoretically evaluated[9,19−22] and experimentally used[10,19−27] to measure rate constants in a medium that contains a fluorescent probe exchanging between two states of different brightness when it reacts with a species of interest. Possible FCS applications to titrations were already addressed for the proton[19,23−27] and the calcium(II) ion.[23]

The FCS titration approach is especially significant. It is noninvasive, and it can thus be performed in living cells[28−30] by using tiny amounts of fluorescent indicators, either permeant or synthesized in vivo (the green fluorescent protein GFP or its mutants, for instance). In addition, FCS may yield local concentrations at micrometer resolution that can be obtained either intrinsically with two-photon excitation or by using a pinhole when FCS relies on one-photon excitation.

As attractive as it is, the FCS titration approach is nevertheless rather constraining (vide infra). In particular, it requires carefully designed fluorescent probes that integrate specific photophysical, thermodynamic, and kinetic requirements. If one excepts pH and pOH jump molecules that exploit the properties of excited states,[31] the kinetic aspect is rather unusual in molecular engineering of fluorescent probes. In contrast, it is crucial here. In fact, FCS opportunities surely merit the work to address such a new challenge.

In the present report, we evaluate FCS to access the local concentration in a reactant $\mathscr{H}$ with a fluorescent reagent $\{\mathscr{AH},\mathscr{A}\}$. In section 2 and in the Supporting Information, we revisit the theoretical treatment of the correlation functions of fluorescence emission in such a situation. In addition to previous analyses,[9,19−22] we examine the following: (i) the observation of the reactivity of the ground or of the excited state of $\{\mathscr{AH},\mathscr{A}\}$ (this point is especially important because those reactivities can considerably differ such as, for instance, in the case of fluorescent pH probes[32−34] that are used for experimental illustration); (ii) the most favorable approximation to access tractable expressions of the correlation functions; (iii) the experimental constraints to access H with FCS. FCS is shown to be a superior tool to measure concentrations of reactive species provided that appropriate fluorescent probes are available: selectivity is at the highest because both the thermodynamics and the kinetics of reaction 1 are used to obtain the reactant concentration.[35] In addition, preliminary calibrations can sometimes even be avoided. To evaluate the preceding theoretical results, section 3 makes use of three fluorescent probes that we recently designed to measure pH in the 3−7 range by ratiometric means.[36,37] We first measure and analyze their kinetics of proton exchange by FCS after two-photon excitation. We then demonstrate that one can use them to efficiently estimate pH around 4−6 by FCS after two-photon excitation without preliminary calibration. Despite this favorable result, we suggest that further improvements will still be necessary to reliably extract pH in unknown media from FCS measurements. Section 4 is devoted to the conclusion.

2. Theoretical Analysis

In FCS, one observes and analyzes the fluctuations of the number of photons $n(\vec{r}, t)$ collected from fluorescent molecules that are contained in a tiny illuminated volume V (typically 1 fL) delimited by focusing a laser beam (see Supporting Information Figure 1S for the presentation of the setup used in the group). Thanks to the intrinsic sensitivity of fluorescence, one can observe very dilute solutions (less than 1 nM) that cause large fluctuations $\delta n(\vec{r}, t)$ around average values $\overline{n(\vec{r})}$: at 1 nM with $V = 1$ fL, $\delta n(\vec{r}, t) \approx \overline{n(\vec{r})}$. A FCS setup generally computes the autocorrelation function of fluorescence emission, defined in eq 2, that gives the time average of the products of

$$G(\tau) = \frac{\langle \delta n(\vec{r}, 0)\, \delta n(\vec{r}, \tau) \rangle}{\overline{n(\vec{r})}\ \overline{n(\vec{r})}} \qquad (2)$$

(5) Diu, B.; Guthmann, C.; Lederer, D.; Roulet, B. *Physique Statistique*; Hermann: Paris, 1989.
(6) Berne, B. J.; Pecora, R. *Dynamic Light Scattering with Applications to Chemistry, Biology, and Physics*; Dover: Mineola, NY, 2000.
(7) van Kampen, N. G. *Stochastic Processes in Physics and Chemistry*, 5th ed.; Elsevier: Amsterdam, 2004.
(8) Magde, D.; Elson, E. L.; Webb, W. W. *Phys. Rev. Lett.* **1972**, *11*, 705−708.
(9) Elson, E. L.; Magde, D. *Biopolymers* **1974**, *13*, 1−27.
(10) Magde, D.; Elson, E. L.; Webb, W. W. *Biopolymers* **1974**, *13*, 29−61.
(11) Thompson, N. L. Fluorescence Correlation Spectroscopy. *Topics in Fluorescence Spectroscopy, Techniques*; Lakowicz, J., Ed.; Plenum Press: New York, 1991; Vol. 1, pp 337−410.
(12) *Fluorescence Correlation Spectroscopy*; Rigler, R., Elson, E. S., Eds.; Springer Series in Chemical Physics; Springer-Verlag, Berlin, 2001.
(13) Elson, E. L. *Traffic* **2001**, *2*, 789−796.
(14) Chen, Y.; Müller, J.-D.; Eid, J.-S.; Gratton, E. In *New Trends in Fluorescence Spectroscopy, Applications to Chemical and Life Sciences*; Valeur, B., Brochon, J.-C., Eds.; Springer Series on Fluorescence, Methods and Applications; Springer: Berlin, 2001; pp 277−296.
(15) Thompson, N. L.; Lieto, A. M.; Allen, N. W. *Curr. Opin. Struct. Biol.* **2002**, *12*, 634−641.
(16) Krichevsky, O.; Bonnet, G. *Rep. Prog. Phys.* **2002**, *65*, 251−297.
(17) Hess, S. T.; Huang, S.; Heikal, A. A.; Webb, W. W. *Biochemistry* **2002**, *41*, 697−705.
(18) Here, we do not consider the situation where at least one reactant is immobilized such as in, for instance: Lieto, A. M.; Cush, R. C.; Thompson, N. L. *Biophys. J.* **2003**, *85*, 3294−3302.
(19) Widengren, J.; Terry, B.; Rigler, R. *Chem. Phys.* **1999**, *249*, 259−271.
(20) Lamb, D. C.; Schenk, A.; Röcker, C.; Scalfi-Happ, C.; Nienhaus, G. U. *Biophys. J.* **2000** *79*, 1129−1138.
(21) Bismuto, E.; Gratton, E.; Lamb, D. C. *Biophys. J.* **2001**, *81*, 3510−3521.
(22) Hom, E. F. Y.; Verkman, A. S. *Biophys. J.* **2002**, *83*, 533−546.
(23) Widengren, J.; Rigler, R. *J. Fluoresc.* **1997**, *7*, 211S-213S.
(24) Widengren, J.; Rigler, R. *Cell. Mol. Biol.* **1998**, *44*, 857−879.
(25) Haupts, U.; Maiti, S.; Schwille, P.; Webb, W. W. *Proc. Natl. Acad. Sci. U.S.A.* **1998**, *95*, 13573−13578.
(26) Schwille, P.; Kummer, S.; Heikal, A. A.; Moerner, W. E.; Webb, W. W. *Proc. Natl. Acad. Sci. U.S.A.* **2000**, *97*, 151−156.
(27) Hess, S. T.; Heikal, A. A.; Webb, W. W. *J. Phys. Chem. B* **2004**, *108*, 10138−10148.
(28) Berland, K. M.; So, P. T. C.; Gratton, E. *Biophys. J.* **1995**, *68*, 694−701.
(29) Schwille, P.; Haupts, U.; Maiti, S.; Webb, W. W. *Biophys. J.* **1999**, *77*, 2251−2265.
(30) Gennerich, A.; Schild, D. *Biophys. J.* **2000**, *79*, 3294−3306.
(31) For a recent reference, see, for instance: Moscovitch, D.; Noivirt, O.; Mezer, A.; Nachliel, E.; Mark, T.; Gutman, M.; Fibich, G. *Biophys. J.* **2004**, *87*, 47−57.
(32) Förster, T. *Z. Elektrochem.* **1950**, *54*, 42−46.
(33) (a) Weller, A. *Z. Elektrochem.* **1952**, *56*, 662−668. (b) Weller, A.; *Z. Phys. Chem. Neue Folge* **1955**, *3*, 238−254. (c) Weller, A. *Z. Phys. Chem. Neue Folge* **1958**, *17*, 224−245.
(34) Schulman, S. G. *Molecular Luminescence Spectroscopy, Methods and Applications*; Wiley-Interscience: New York, Chichester, Brisbane, Toronto, Singapore, 1988; Part 2.
(35) Winkler-Oswatitsch, R. W.; Eigen, M. *Angew. Chem., Int. Ed. Engl.* **1979**, *18*, 20−49.
(36) Charier, S.; Ruel, O.; Baudin, J.-B.; Alcor, D.; Allemand, J.-F.; Meglio, A.; Jullien, L. *Angew. Chem., Int. Ed. Eng.* **2004**, *43*, 4785−4788.
(37) Charier, S.; Ruel, O.; Baudin, J.-B.; Alcor, D.; Allemand, J.-F.; Meglio, A.; Jullien, L.; Valeur, B. *Chem. Eur.−J.*, accepted for publication.

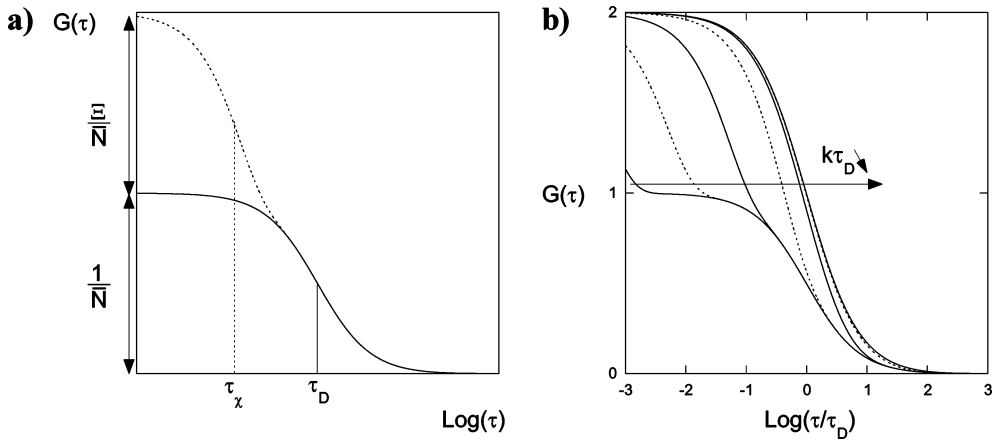

Figure 1. (a) Principle of extraction of a reactant concentration from an autocorrelation curve recorded from a reactive mixture (dotted line). Fitting with eq 3 provides $\bar{N}$ and τ_D from the term $G_D(\tau)$ related to the diffusion (solid line), and Ξ and τ_χ from the term related to chemistry. After calibration of the beam waist, $\bar{N}$ and τ_D yield the total concentration C in fluorescent probe $\{\mathcal{AH},\mathcal{A}\}$ on one hand and either the $\{\mathcal{AH},\mathcal{A}\}$ diffusion coefficient d or the local viscosity on the other hand. In contrast, Ξ depends on $\bar{H}$, K, and the relative brightness $Q = (\mathcal{Q}_{\mathcal{AH}}/\mathcal{Q}_{\mathcal{A}})$, whereas τ_χ depends on $\bar{H}$, K, and one of the rate constants k or k'. If K and Q are known, Ξ yields $\bar{H}$. If one rate constant, k or k', is additionally known, $\bar{H}$ can be also extracted from τ_χ. (b) Theoretical dependence of the autocorrelation function $G(\tau)$ on adimensional time τ/τ_D as calculated from eq 3 for different values of $k\tau_D$: 10^3, 10^2, 10, 1, 10^{-1}, 10^{-2}, and 10^{-3}. Parameter values for the calculation are $\bar{N} = 1$, $\omega = 10$, $\bar{H} = K$, and $Q = \infty$.

the intensity fluctuations normalized by the product of the average intensities.

***G*(τ) for a Reactive System with Three Reactants.** To extract the relevant thermodynamic and kinetic parameters from FCS data, the experimental autocorrelation function $G(\tau)$ has to be fitted with theoretical expressions. When the reactive system involves more than two reactants, assumptions are required to obtain approximate analytical expressions of the autocorrelation function $G(\tau)$ (see Supporting Information).

We first use the steady-state approximation: the fastest processes are relaxed at the time scale of the slowest ones. Then, the typical nanosecond range for the lifetime of singlet excited states as well as the hundred-nanoseconds time resolution of the autocorrelator in a current FCS setup led us to conclude that, although relying on the analyses of the fluctuations of the fluorescence intensity from excited states, FCS reveals the reactivity of virtual averaged species that involve both the ground and the excited states (see Supporting Information). In fact, the autocorrelation functions essentially contain rate and thermodynamic constants associated with ground states in most encountered experimental situations (see Supporting Information). This conclusion is especially significant because the rate constants of chemical reactions can sometimes be considerably altered by the nature, ground or excited, of the state (rate constants for proton exchange reactions can be changed by 10 orders of magnitude, for instance).[32−34]

We are now interested in getting $G(\tau)$ for a system submitted to reaction 1. k and k' designate the rate constants of the forward and backward processes, and $K = k/k'$, the equilibrium constant of reaction 1. $\bar{H}$ is the average concentration in $\mathcal{H}$ in the illuminated volume V, and $C = A\bar{H} + A$. In relation with titrating $\mathcal{H}$ with a fluorescent reagent $\{\mathcal{AH},\mathcal{A}\}$ in the most general case, we assume that $\mathcal{H}$ is not fluorescent. In addition, we consider that the diffusion coefficients of $\mathcal{AH}$ and $\mathcal{A}$ are identical and equal to d. This approximation is satisfactory as long as $\mathcal{H}$ is small enough. For instance, the acidic and basic states of a pH indicator exhibit similar shape and size. In addition, the small difference in charge between both states is not expected to alter the diffusion coefficient by different coupling with the cloud of the counterions at any relevant ionic strength.[1]

Lamb et al. introduced a simple approximate analytical expression of $G(\tau)$ when $C \ll \bar{H}$.[20] In FCS, this condition should be often fulfilled because sensitive detectors such as avalanche photodiodes make measurements possible down to the nanomolar range in $\{\mathcal{AH},\mathcal{A}\}$: a large range of $\mathcal{H}$ concentrations is thus accessible (see Supporting Information). Then,

$$G(\tau) = G_D(\tau)\,[1 + \Xi\, e^{-(\tau/\tau_\chi)}] \tag{3}$$

with

$$G_D(\tau) = \frac{1}{\bar{N}}\left(1 + \frac{\tau}{\tau_D}\right)^{-1}\left(1 + \frac{\tau}{\omega^2\tau_D}\right)^{(-1/2)} \tag{4}$$

and

$$\Xi = \frac{K}{\bar{H}}\left(\frac{Q-1}{Q + \frac{K}{\bar{H}}}\right)^2 \tag{5}$$

where $\bar{N} = CV$, $\tau_D = \omega_{xy}^2/(4d\nu)$, $\omega = (\omega_z/\omega_{xy})$, and $Q = \mathcal{Q}_{\mathcal{AH}}/\mathcal{Q}_{\mathcal{A}}$ designate, respectively, the average number of $\{\mathcal{AH},\mathcal{A}\}$ molecules contained in the illuminated volume V, the diffusion time of $\{\mathcal{AH},\mathcal{A}\}$ through the beam waist described as 3D-Gaussian with ω_{xy} diameter and ω_z height (ν is equal to 1 for one-photon excitation and to 2 for two-photon excitation), the aspect ratio of the 3D-Gaussian volume V, and the ratio of the effective brightness, $\mathcal{Q}_{\mathcal{AH}}$ and $\mathcal{Q}_{\mathcal{A}}$, associated to the states $\mathcal{AH}$ and $\mathcal{A}$. $G(\tau)$ is the product of the diffusive term, $G_D(\tau)$, and of the term in square brackets associated with the chemical relaxation. Figure 1a displays a typical prediction for the $G(\tau)$ function from eq 3. In particular, Figure 1a makes explicit the significance of $\bar{N}$ and Ξ and of τ_D and τ_χ to, respectively, determine the amplitude and the time dependence of the $G(\tau)$ function.

Measuring Reactant Concentrations by FCS. In the following, we assume that $C \ll \overline{H}$ to be able to use the simple analytical expression (eq 3) to extract the concentration $\overline{H}$ sought from correlation functions of $\{\mathcal{AH},\mathcal{A}\}$ fluorescence emission.

A. General Case. As shown in Figure 1a, fitting the experimental data with eq 3 should provide $\overline{N}$ and τ_D from the term $G_D(\tau)$ related to the diffusion and Ξ and τ_χ from the term related to chemistry.[38]

A fruitful interpretation of $\overline{N}$ and τ_D requires a preliminary calibration of the illuminated volume V. This can be done by using a reference fluorophore such as fluorescein at a known concentration. Then, $\overline{N}$ and τ_D yield the total concentration in $\{\mathcal{AH},\mathcal{A}\}$, $C = \overline{N}/V$, on one hand and the diffusion coefficient of $\{\mathcal{AH},\mathcal{A}\}$, $d = \omega_{xy}^2/(4\nu\tau_D)$, on the other hand.

In contrast, Ξ depends on $\overline{H}$, on K, and on the relative brightness Q, whereas τ_χ depends on $\overline{H}$, on K, and on one of the rate constants, k or k' ($\tau_\chi \approx [k + k'\overline{H}]^{-1}$ in the present region of approximation). If K and $\overline{H}$ are known, it is possible to determine the rate constants k and k' from the measurement of τ_χ. Conversely, if K and Q are known, Ξ yields $\overline{H}$. If one rate constant, k or k', is additionally known, $\overline{H}$ can also be extracted independently from τ_χ.

As far as Ξ analysis only is concerned, FCS satisfactorily compares with ratiometric methods because both the thermodynamic (K) and the photophysical (Q) information is required to extract $\overline{H}$ from the experimental data. FCS alternatively yields $\overline{H}$ from τ_χ if the thermodynamic and rate constants of reaction 1 are known. Under such a condition, FCS should be at the most selective because $\overline{H}$ measurement relies on both thermodynamic and kinetic data from reaction 1.[35] This point is a major advantage if one deals with a mixture of species that can interact with the fluorescent indicator.

As a general conclusion, FCS provides more observables than the classical methods evoked in the Introduction to measure $\overline{H}$. Nevertheless, preliminary calibrations are still required in the most general case.

B. "Calibration-Free" Approach. In fact, FCS reveals its definitive advantages only after proper design of the $\{\mathcal{AH},\mathcal{A}\}$ fluorescent reagent. As an example related to the experimental part of the present work, we first assume that either $\mathcal{Q}_{\mathcal{AH}}$ or $\mathcal{Q}_{\mathcal{A}}$ is equal to zero ($\mathcal{AH}$ or $\mathcal{A}$ appears nonfluorescent *on the detecting channels*). For instance, reaction 1 can be accompanied by the quenching or the shift of the emission of the fluorescent reagent. Second, we suppose that the reaction of $\mathcal{A}$ with $\mathcal{H}$ is limited by the diffusion (vide infra). Then, a good order of magnitude of the rate constant k' can be derived from the respective diffusion coefficients of $\mathcal{A}$ (d) (extracted from the diffusive term $G(\tau)$ in eq 4) and $\mathcal{H}$ (D):

$$k' \approx 4\pi N_A(d + D)a \tag{6}$$

where N_A and a, respectively, designate the Avogadro number and a captured length in the 1 nm range.[39] If k' is known, both Ξ and τ_χ only depend on $\mathcal{H}$ and K. Consequently, the simultaneous measurement of Ξ and τ_χ should now yield, without any preliminary calibration, not only the desired $\mathcal{H}$ concentration but also the value of the thermodynamic constant K.

Constraints on Measuring Concentrations by FCS. The preceding paragraph suggests that FCS could be extremely attractive to measure concentrations: this noninvasive technique can yield local concentrations at the micrometer resolution without calibration in the best cases. In fact, its impact will strongly depend on the proper design of fluorescent reagents. This section examines different types of constraints on accessing reactant concentrations by FCS.

A. Amplitude of Ξ. To be used for analysis, the amplitude of the chemical term, Ξ, must be large enough (see eq 3). Figure 2a displays the dependence of Ξ on $\log_{10}(K/\overline{H})$ and on $\log_{10} Q$. In the following, we assume the solutions to be ideal and we denote $\mathrm{pH} = -\log_{10} \overline{H}$ and $\mathrm{p}K = -\log_{10} K$ in relation to the following experimental illustration.

FCS does not reveal the occurrence of reaction 1 when the brightnesses of $\mathcal{AH}$ and $\mathcal{A}$ are identical: For $Q = 1$, $\Xi = 0$ over the whole range of pH−pK. Ξ is appreciably large only in symmetrically related zones of the two quadrants in the (Q, pH−pK) space ($\Xi \approx 1$ under our experimental conditions).[40] In these two zones, the large value of Ξ is associated with occurrences of transitions from the darkest state that is present in the largest amount to the minor brightest state.

B. Statistical Accuracy. In practice, the intrinsic noise of the experimental setup limits the statistical accuracy of FCS experiments. In fact, FCS experiments provide reliable information related to the fluorescent probe only when $\overline{N}$ is larger than the equivalent number of molecules, $\overline{N'}$, associated to the background fluorescence.[41]

If Ψ and Ψ_{min}, respectively, designate the photon fluxes from the illuminated volume V that originates from the $\overline{N}$ fluorescent probe molecules and that gives rise to a signal equal to the intrinsic noise at the detecting unit, then

$$\frac{\overline{N'}}{\overline{N}} = \frac{\Psi_{min}}{\Psi} = \frac{1 + \dfrac{K}{\overline{H}}}{\varphi\overline{N}\mathcal{Q}_{\mathcal{A}}\left(Q + \dfrac{K}{\overline{H}}\right)}\Psi_{min} \tag{7}$$

where φ is the photon collection factor of the setup. Note that $\overline{N'}$ depends on the pH-dependent average brightness of the fluorescent probe.

The preceding subsection emphasized that the measurement of reactant concentrations by FCS can only be performed when the brightest state is in a low amount. Unfortunately, the gain in the fluctuation amplitude is counterbalanced by a corresponding drop of statistical accuracy due to the low average brightness under such conditions. For instance, when $Q \gg (K/\overline{H}) \gg 1$, increasing the pH−p$K$ by one unit also increases $\overline{N'}$ by a factor of 10 because $((\mathcal{Q}_{\mathcal{A}}/1) + (K/\overline{H}))(Q + (K/\overline{H})) \approx (\mathcal{Q}_{\mathcal{AH}}/(K/\overline{H}))$.

(38) ω does not significantly affect $G(\tau)$ and cannot be reliably extracted from the fit. See ref 14.

(39) Berry, R. S.; Rice, S. A.; Ross, J. *Physical Chemistry*, 2nd ed.; Oxford University Press: Oxford, U.K., 2000.

(40) For a given relative brightness, Q, two different $\overline{H}$ values give noticeably the same Ξ value; in principle, it should not be possible to extract pH−pK from Ξ without ambiguity. In fact, the constraint on the intensity of fluorescence emission should forbid the observation of the branch attached to pH values significantly departing from pK (vide infra).

(41) Koppel, D. E. *Phys. Rev. A* **1974**, *10*, 1938−1945.

The condition $\overline{N} \geq \overline{N'}$ is equivalent to

$$\left(\frac{1}{1+Q}\right)\left(\frac{Q+\frac{K}{\overline{H}}}{1+\frac{K}{\overline{H}}}\right) \geq \frac{\Psi_{\min}}{\varphi\overline{N}(\mathcal{Q}_{\mathcal{MH}}+\mathcal{Q}_{\mathcal{M}})} \equiv \alpha^{-1} \qquad (8)$$

Figure 2b displays for different values of α the domain in which eq 8 is fulfilled in the (pH−pK, $\log_{10} Q$) space (α ≈ 10 under our experimental conditions). Significant experiments can be essentially performed in the two quadrants, $Q > 1$ and pH < pK and $Q < 1$ and pH > pK.

To enlarge the extent of the relevant domain, one could first imagine increasing $\overline{N}$. Unfortunately, this would reduce the total amplitude of the FCS autocorrelation function that inversely depends on $\overline{N}$ (see eqs 3 and 4). With the currently available detecting systems, $C \approx 10-10^3$ nM seems rather optimal. In principle, one could also improve the collection factor and the instrumental response to enlarge φ. Eventually, one can increase the brightness of the fluorescent probe by engineering its absorption and emission properties.

Comparison between Figure 2a and 2b is useful to analyze the domains in which the measurement of reactant concentrations can be performed by FCS. Figure 2c displays the typical zone that can be investigated with our experimental setup by using the following fluorescent pH probes. The best results should be eventually obtained in the range pH ≈ pK.

C. Kinetic Window. In fact, stringent kinetic constraints also have to be taken into account. Figure 1b illustrates the theoretical evolution of the autocorrelation function $G(\tau)$ as a function of the normalized time τ/τ_D for different relaxation times τ_χ of reaction 1; in relation to the preceding paragraphs, the calculations were performed at pH = pK, where $\tau_\chi = 1/(2k) = 1/(2k'\overline{H})$.

As long as $\tau_\chi \leq \tau_D$ (i.e., $k\tau_D \geq 1$), the autocorrelation function exhibits two thresholds at τ_χ and τ_D that are associated with the regression of the fluctuations from chemical and diffusional origins, respectively. The amplitudes of these two contributions are, respectively, equal to $\Xi/\overline{N}$ and $1/\overline{N}$ (see also Figure 1a). In the corresponding region, both thermodynamic and kinetic information on reaction 1 can be extracted from the autocorrelation function. In contrast, when $\tau_\chi \gg \tau_D$ (i.e., $k\tau_D \ll 1$), the autocorrelation function exhibits only one threshold at τ_D with an amplitude that is equal to $(1 + \Xi)/\overline{N}$. As anticipated from the absence of a chemical reaction at the time scale of the diffusion through the beam waist in the corresponding region, this behavior corresponds to a nonreactive mixture of $\mathcal{MH}$ and $\mathcal{M}$: only the thermodynamic constant of reaction 1 can be extracted from the autocorrelation function.

In relation to measuring the concentration $\overline{H}$ by FCS, the region $\tau_\chi \leq \tau_D$ is more favorable because both kinetic and thermodynamic information can be exploited. To reach this region, it is possible to play with τ_D or with τ_χ. From an instrumental point of view, it is possible to enlarge τ_D by playing with ω_{xy}. In relation to the engineering of the fluorescent probe, it is difficult to tune τ_D because the diffusion coefficient of the fluorescent probe is only poorly dependent on its structure in the limit of acceptable ranges of size. In fact, τ_D for "small" molecules under typical conditions can be hardly larger than 1 ms with one-photon excitation FCS and 0.1 ms with two-photon excitation FCS. In contrast, molecular design of the fluorescent probe should favor the increase of k' to reduce τ_χ as much as possible at pH = pK.

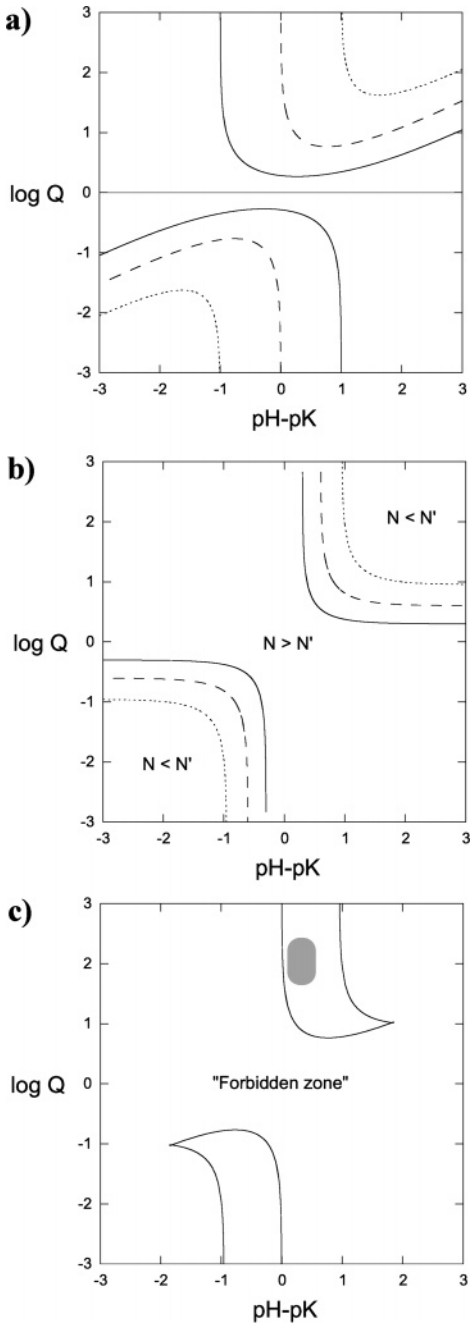

Figure 2. (a) Contour plot of the amplitude Ξ of the chemical term in the autocorrelation function $G(\tau)$ on pH−pK and log Q. Solid line: $\Xi = 0.1$. Dashed line: $\Xi = 1$. Dotted line: $\Xi = 10$. (b) Manifold $\overline{N} = \overline{N'}$ in the (pH−pK, log Q) space for different values of the α parameter. Solid line: $\alpha = 3$. Dashed line: $\alpha = 5$. Dotted line: $\alpha = 10$. (c) Combined diagram picturing the zones where proton concentration can be measured by FCS with the present pH fluorescent probes and with our experimental setup. The gray zone displays the domain in which experiments were performed in the present study.

Nevertheless, there is also a lower limit to the accessible relaxation time τ_χ that is fixed by the temporal resolution τ_{cor} of the autocorrelator ($\tau_{cor} = 0.1$ μs in the present FCS setup). At the τ_{cor} time scale, the fluorescent probe exchanging between the acidic and the basic states behaves as a single species and

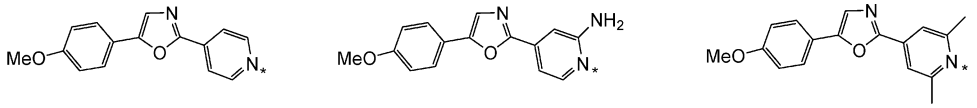

Figure 3. Fluorescent pH indicators that were used in the present study: **4-PYMPO**, **4-PYMPO−NH$_2$**, and **4-PYMPOM**. The relevant protonation site in the considered pH range is indicated with an asterisk.

chemistry is no longer visible in FCS if $\tau_\chi < \tau_{cor}$. In fact, the autocorrelation function only contains the information related to the diffusion of the fluorescent probe: it is impossible to extract the concentration $\overline{H}$ by FCS. This type of situation is illustrated in Figure 1b for $k\tau_D = 10^3$.

As a conclusion, the preceding paragraphs emphasize that the measurement of reactant concentrations by FCS is attractive but rather constraining. Ideally, a good fluorescent reagent $\{\mathscr{AK},\mathscr{A}\}$ would (i) have a thermodynamic constant K in the $\overline{H}$ working range (control of Ξ amplitude), (ii) be at the brightest (control of the amplitude of fluorescence emission), (iii) exhibit a major change of fluorescence intensity upon reaction 1 (control of Ξ amplitude), (iv) yield a relaxation time τ_χ in the 1−100 μs range (constraint on the kinetic window), and (v) possibly react with $\mathscr{K}$ under control of diffusion (to avoid any calibration).

3. Application to pH Measurement by FCS after Two-Photon Excitation

The proton is probably the first reactant one could imagine to titrate by FCS.[19,23,24] Beyond the intrinsic significance of the proton, proton exchange reactions provide a wide range of thermodynamic and kinetic behaviors allowing one to find appropriate fluorescent indicators. In addition, the mechanisms governing the proton exchange reactions are rather simple and were already thoroughly examined.[42,43]

Presentation of the Fluorescent pH Indicators. We recently reported on a series of fluorescent probes for dual emission wavelength pH measurement that work in the biologically relevant 4−7 pH range.[36,37] These probes were additionally designed to fulfill, as much as possible, the requirements exposed in the preceding paragraph when two-photon excitation is used for FCS. In fact, this excitation mode is especially adapted to perform local investigations because of its intrinsic limitation of the excitation volume.[14,28]

A. Design. The thermodynamic and kinetic issues of the fluorescent probe were addressed as follows.

We ideally sought a fluorescent pH indicator that would exhibit a chemical relaxation time such that $\tau_{cor} \le \tau_\chi \le \tau_D$ with $\tau_D < 100$ μs (vide supra). We engineered $\tau_\chi \approx 10$ μs. We first considered that the reaction of a base with a proton is most often controlled by diffusion.[42,43] As explained above, this feature is especially favorable here. Respectively, denoting $\mathscr{AK}$ and $\mathscr{A}$ as the acidic and the basic states of the fluorescent pH indicator and denoting $\mathscr{K}$ as the proton, we sought $k' \approx 10^{10}$ M^{-1} s^{-1}.[42,43] In addition, we decided to work at pH = pK = pK_a (vide supra) where K_a designates the protonation constant of the fluorescent pH indicator. Taking into account that $\tau_\chi = 1/(2k) = 1/(2k'\overline{H}) \approx 10$ μs at pH = pK_a, we got pH = p$K_a \approx$ 5. Thus, we designed fluorescent pH indicators with a pK_a between 4 and 6 that would not exhibit any significant steric hindrance around the basic site to maintain the diffusion-limited rate constant for its protonation.

From a photophysical point of view, we additionally favored pH indicators exchanging between two strongly fluorescent states, $\mathscr{AK}$ and $\mathscr{A}$, with shifted emission spectra. First, this allowed us to tune the respective brightness of the exchanging states by changing the excitation wavelength and by using appropriate filters; this may find applications in dual-color fluorescence cross-correlation spectroscopy.[22,44] In addition, this feature provided a way to directly access pH from a ratiometric analysis of the fluorescence emission from the acidic and basic states of the pH indicator. In the present series of experiments, this was favorable because it is impossible to reliably measure $\overline{H}$ at neutral pH with the glass electrode of a pH meter in the absence of supporting salt at the corresponding concentrations.

Figure 3 displays the three tailored water-soluble fluorescent pH indicators that we eventually retained: **4-PYMPO**, **4-PYMPO−NH$_2$**, and **4-PYMPOM**.[36,37]

B. Photophysical Properties and Protonation Constants. In relation to the present work, the main relevant photophysical properties of the three retained pH indicators are displayed in Figure 4 and summarized in Table 1. Their absorption and emission features made them appropriate to perform FCS experiments after two-photon excitation. The typical order of magnitude of their maximal peak two-photon absorptivities in the 700−900 nm range is 60 ± 10 GM (1 GM = 10^{-50} cm^4 s (photon·molecule)$^{-1}$). They additionally exhibit a strong fluorescence emission (quantum yield of fluorescence Φ_F up to 0.8) in the 400−600 nm range for both acidic and basic states of the three pH indicators.

The ground-state pK_a of the present pH indicators is located in the 4−6 range (Table 1). In relation to the preceding paragraph, they should be appropriate to perform kinetic experiments and pH measurements relying on FCS after two-photon excitation. As explained in the Theoretical Analysis section and in the Supporting Information, here, it is important to note that FCS reveals the reactivity of the ground state of the present pH probes despite a large shift of their pK_a upon light excitation.[37]

C. Diffusion Coefficients. To evaluate the intrinsic diffusion coefficients of the fluorescent pH indicators, one can analyze the autocorrelation functions from their solutions at a pH largely departing from their pK_a. Under such conditions, the chemical contribution in eq 3 reduces to one (i.e., $\Xi = 0$). Figures 5a and 6a,b display typical experimental FCS autocorrelation curves for solutions of **4-PYMPO**, **4-PYMPO−NH$_2$**, and **4-PYMPOM** at a pH significantly lower than their pK_a, where the acidic state is essentially present. The fit according to eq 4 is satisfactory for all compounds. The extracted data, $G_D(0)$ and

(42) Eigen, M. *Angew. Chem.* **1963**, *75*, 489−508.
(43) Eigen, M.; Kruse, W.; Maas, G.; de Mayer, L. In *Progress in Reaction Kinetics;* Porter, G., Ed.; Pergamon Press: Oxford, London, Edinburgh, New York, Paris, Frankfurt, 1964, Vol. 2; pp 287−318.
(44) Schwille, P.; Meyer-Almes, F.-J.; Rigler, R. *Biophys. J.* **1997**, *72*, 1878−1886.

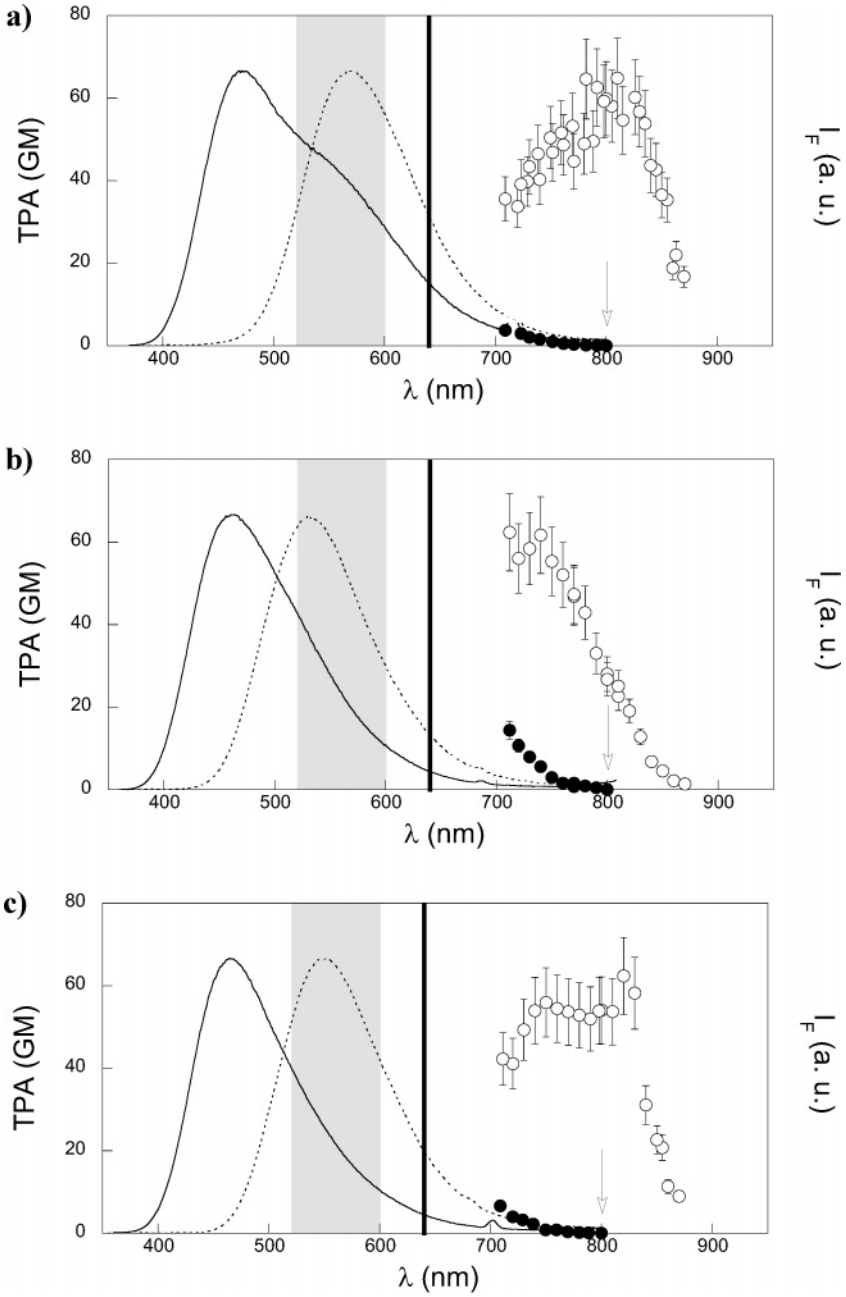

Figure 4. Photophysical properties of the present fluorescent pH indicators that are relevant for FCS after two-photon excitation. Two-photon excitation spectra $\delta(\lambda^{(2)})$ and normalized steady-state fluorescence emission $I_F(\lambda^{(1)})$ after one-photon excitation (acidic state = dotted line and empty disks; basic state = solid line and filled disks). (a) **4-PYMPO**; (b) **4-PYMPO−NH$_2$**; (c) **4-PYMPOM**. Solvent: Britton-Robinson buffer[45] (acetic acid, boric acid, phosphoric acid) at 0.1 M. T = 293 K. The characteristics of dichroic mirror (thick line) and filters (gray zone) used for spectral separation of the emission light are also indicated, as well as the excitation wavelength (arrow); such conditions were used to adopt $Q = \infty$ for fitting. Adapted from ref 37.

τ_D, can be analyzed after calibration of the illuminated volume V and of the beam waist by recording the FCS autocorrelation curve from a solution of a reference fluorophore such as fluorescein at a known concentration. The extracted $G_D(0)$ value reasonably conformed to the expectation based on the nominal concentrations. In addition, the fits, respectively, provided 370 ± 30, 470 ± 30, and 440 ± 30 $\mu m^2\ s^{-1}$ for the diffusion coefficients of the acidic states of **4-PYMPO**, **4-PYMPO−NH$_2$**, and **4-PYMPOM** at 293 K. Such values satisfactorily compare with the diffusion coefficient of fluorescein that is a slightly larger molecule than the present probes; under similar conditions, the diffusion coefficient of fluorescein is 300 ± 30 $\mu m^2\ s^{-1}$.[14]

In the case of **4-PYMPO**, we also measured the diffusion coefficient at a pH much above its pK_a: at pH = 12, we found a value of 400 ± 30 $\mu m^2\ s^{-1}$ at 293 K. The similarity between the values obtained for the acidic and basic states is in agreement with the similarity of the size and the shape of both states. This observation pushed us to adopt, for all the investigated pH indicators, the value of the diffusion coefficient that was measured in the acidic state where the brightness was at the largest under our experimental conditions.

D. Rate Constants for Proton Exchange. D.1. Design of the Experiments. The Theoretical Analysis section suggested that working at pH = pK_a is the most favorable to reveal the kinetic behavior of a fluorescent pH probe by FCS. Nevertheless,

Table 1. Photophysical Properties, Protonation Constants (p$K_a \pm 0.1$), Diffusion Coefficients ($d \pm 30$ μm^2 s^{-1}), and Rate Constants for Proton Exchange ($k_{13} \pm 10\%$ s^{-1} and $k_{31} \pm 10\%$ M^{-1} s^{-1}) of **4-PYMPO**, **4-PYMPO-NH$_2$**, and **4-PYMPOM**[a]

	4-PYMPO[b]	4-PYMPO–NH$_2$[b]	4-PYMPOM[b]	4-PYMPOM[c]
$\lambda^{(1)}_{max}$ (ϵ_{max})[d]	390 (21)/332 (21)[e]	355 (23)/326 (19)[e]	380 (19)/330 (17)[e]	382 (11)/330 (14)
$\lambda^{(1)}_{em}$ [Φ_F][f]	569 [0.3]/472 [0.5][e]	530 [0.7]/465 [0.8][e]	550 [0.5]/465 [0.8][e]	549 [0.4]/444 [0.8]
$\lambda^{(2)}_{max}$ ($\delta_{2,max}$)[g]	800 (65)/710 (5)[e]	710 (60)/710 (15)[e]	800 (60)/710 (10)[e]	
p$K_a \pm 0.1$	4.3[e]	5.7[e]	5.7[e]	5.3
d	370	470	440	690
$10^{-4}k_{13}$	80	3	3	16
$10^{-10}k_{31}$	1.2	1.3	1.5	3.2

[a] $T = 293$ K. [b] Solvent/water. [c] Solvent: acetonitrile/water 60:40 (v/v). [d] Maxima of single-photon absorption $\lambda^{(1)}_{max}$ (nm). Molar absorption coefficients for single-photon absorption at $\lambda^{(1)}_{max}$, ϵ_{max} ($\pm 10\%$; mM^{-1} cm^{-1}). [e] From ref 37. [f] Maxima of steady-state fluorescence emission $\lambda^{(1)}_{em}$ (nm). Quantum yields of fluorescence Φ_F ($\pm 5\%$). [g] Maxima of two-photon excitation spectra $\lambda^{(2)}_{max}$ (nm) in the investigated 700−900 wavelength range. Two-photon excitation cross sections at $\lambda^{(2)}_{max}$, $\delta_{2,max}$ ($\pm 20\%$; GM, 1 GM = 10^{-50} cm^4 s (photon·molecule)$^{-1}$).

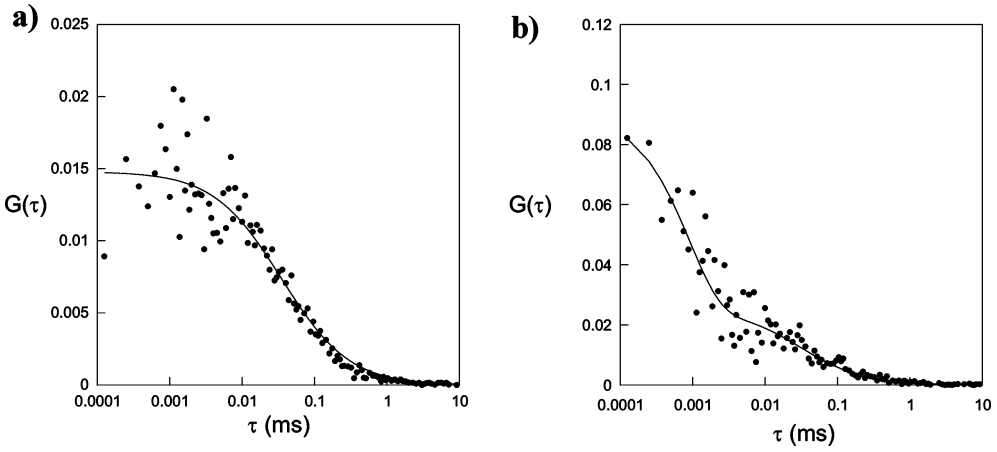

Figure 5. FCS autocorrelation curves recorded at 293 K from solutions of **4-PYMPO** ($\lambda^{(2)}_{exc} = 800$ nm). (a) pH = 2.0. The fit according to eq 4 yields $\overline{N}/V = 110 \pm 10$ nM and $d = 370 \pm 30$ μm^2 s^{-1}. (b) pH = 4.6. Using $d = 370 \pm 30$ μm^2 s^{-1} and p$K_a = 4.3$, the fit with eq 3 yields $\overline{N}/V = 75 \pm 10$ nM, pH $= 4.70 \pm 0.05$, and $\tau_{13} = 0.9 \pm 0.1$ μs.

the analysis of the kinetic information from the FCS autocorrelation function requires a careful examination here. In fact, the exchange between the acidic $\mathcal{AH}$ and basic $\mathcal{A}$ states of a fluorescent pH indicator involves more than one chemical reaction, 1, and three components. The relevant minimal mechanism already implies three chemical reactions and five components (Figure 7a).[42,43,46] In the presence of a second acid−base nonfluorescent couple $\{\mathcal{YH},\mathcal{Y}\}$ such as a buffer,[19,23,25−27] the minimal mechanism of proton exchange even contains six chemical reactions and seven components (Figure 7b).[42] In such a complicated dynamical system, a numerical approach could be required to extract rate constants from the experimental autocorrelation function. In fact, much simplification results from (i) considering that only the chemical reactions that involve brightness alterations can be visualized with FCS (in relation to Figure 7b, the relevant reactive channels with exchange between $\mathcal{AH}$ and $\mathcal{A}$ are 13, 23, and 33′) and (ii) applying a simplifying assumption that was already fruitfully used above: at low concentration in a fluorescent pH indicator, the concentration of most chemical species is independent of the occurrences of the conversions between the $\mathcal{A}$ and $\mathcal{AH}$ states and diffusion and chemistry are no longer correlated (see Supporting Information).

To address which relevant reactive channel had to be taken into consideration for the FCS analysis, we first noticed that, in a closed system submitted to the reactions displayed in Figure 7b, the four conservation laws (conservation of $\{\mathcal{AH},\mathcal{A}\}$ is $A_{tot} = \overline{AH} + \overline{A}$, conservation of $\{\mathcal{YH},\mathcal{Y}\}$ is $Y_{tot} = \overline{YH} + \overline{Y}$, conservation of oxygen is $O_{tot} = \overline{H_2O} + \overline{OH}$, and the electroneutrality) imply only three independent processes.[47] In FCS, the chemical relaxation only manifests itself by three noninfinite relaxation times and it is essentially governed by the three fastest exchange processes displayed in Figure 7b. In relation to our experiments that involved fluorescent pH indicators with p$K_a(\mathcal{AH}/\mathcal{A}) \approx 5$, we considered two different situations.

In the first situation, a diluted strong acid with p$K_a(\mathcal{YH}/\mathcal{Y}) < 0$ fixes the pH in the 4−6 ([p$K_a(\mathcal{AH}/\mathcal{A}) - 1$; p$K_a(\mathcal{AH}/\mathcal{A}) + 1$]) range. First, the rate constants for proton transfer between two acid−base couples are generally limited by diffusion when transfer occurs from the strongest acid to the strongest base.[42] Then, one can derive orders of magnitude for the τ_{ij} associated to each reaction (see Supporting Information Table 1S; case 1). The three smallest relaxation times are $\tau_{13'}$, τ_{12}, and τ_{13} with $\tau_{13'} \ll \tau_{12} < \tau_{13}$. Second, H is essentially equal to $\overline{H}$ beyond the $\tau_{13'}$ time scale. Indeed, channels 12 and 13 do not involve considerable amounts of protons at the 10^{-4}−10^{-6} M relevant

(45) Frugoni, C. *Gazz. Chim. Ital.* **1957**, *87*, 403−407.
(46) Here, one here assumes that the solution is dilute enough to neglect the reaction

$$\mathcal{AH} + A \rightleftharpoons A + \mathcal{AH}$$

(47) Lemarchand, H.; Guyot, F.; Jousset, L.; Jullien, L. *Thermodynamique de la Chimie*; Hermann: Paris, 1999.

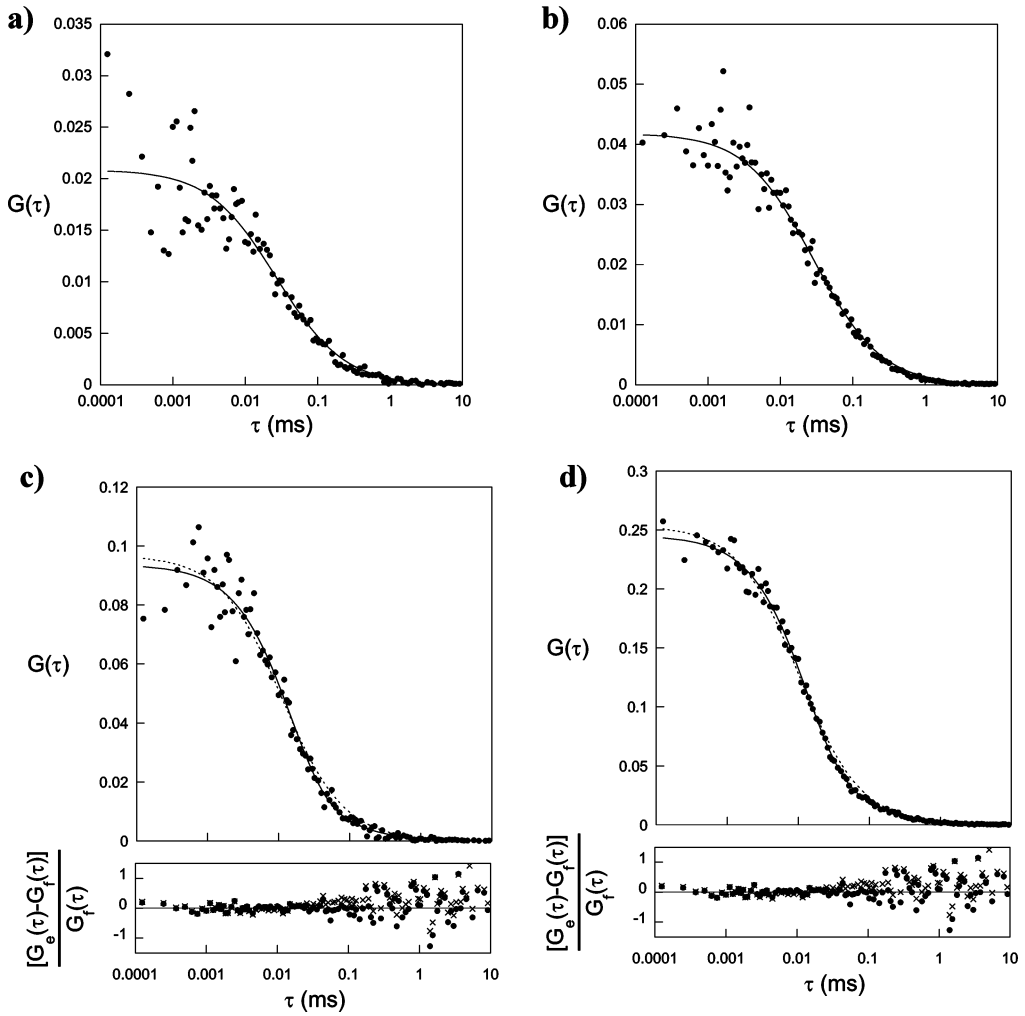

Figure 6. FCS autocorrelation curves recorded at 293 K from solutions of **4-PYMPO−NH$_2$** (a and c) or of **4-PYMPOM** (b and d) ($\lambda_{exc}^{(2)} = 800$ nm). (a) pH = 2.0. The fit according to eq 4 yields $\overline{N}/V = 80 \pm 10$ nM and $d = 470 \pm 30$ μm^2 s^{-1}. (b) pH = 2.0. The fit according to eq 4 yields $\overline{N}/V = 40 \pm 10$ nM and $d = 440 \pm 30$ μm^2 s^{-1}. (c) pH = 6. Using $d = 470 \pm 30$ μm^2 s^{-1} and p$K_a = 5.7$, the fit with eq 3 (solid line) yields $\overline{N}/V = 70 \pm 10$ nM, pH = 6.0 ± 0.1, and $\tau_{13} = 25 \pm 1$ μs. (d) pH = 6. Using $d = 440 \pm 30$ μm^2 s^{-1} and p$K_a = 5.7$, the fit with eq 3 (solid line) yields $\overline{N}/V = 20 \pm 5$ nM, pH = 5.9 ± 0.1, and $\tau_{13} = 20 \pm 1$ μs. In (c) and (d), the fit with eq 4 is displayed with the dotted line and with the cross markers in the analysis of the residues.

concentrations in $\mathscr{YH}$ if $C < 1$ μM. Here, FCS reveals the kinetics of reaction 13. The approximate expression of the autocorrelation function becomes

$$G(\tau) = G_D(\tau)\left[1 + \frac{K_{13}}{\overline{H}}\left(\frac{Q-1}{Q + \frac{K_{13}}{\overline{H}}}\right)^2 e^{-(\tau/\tau_{13})}\right] \qquad (9)$$

in relation to the notations introduced in Figure 7b ($\tau_{13} = [k_{13} + k_{31}(\overline{H} + \overline{A})]^{-1} \approx [k_{13} + k_{31}\overline{H}]^{-1}$).

In the second situation, a buffer with p$K_a(\mathscr{YH}/\mathscr{Y}) \approx 5$ at a significant concentration (typically above 10 mM) is used to fix the pH in the 4−6 range. The three smallest relaxation times are now $\tau_{13'}$, $\tau_{23'}$, and $\tau_{33'}$ (see Supporting Information Table 1S; case 2). $\tau_{33'} = [k_{33'}(\overline{A} + \overline{YH}) + k_{3'3}(\overline{AH} + \overline{Y})]^{-1} \approx [k_{33'}\overline{YH} + k_{3'3}\overline{Y}]^{-1}$ is always the smallest among the three. Fluctuation amplitudes in concentrations of $\mathscr{YH}$ and $\mathscr{Y}$ can be neglected under the present experimental conditions. One eventually notices that $\overline{Y} \gg \overline{AH}$ and $\overline{YH} \gg \overline{A}$. The approximate expression of the autocorrelation function is now

$$G(\tau) = G_D(\tau)\left[1 + \frac{\overline{Y}}{K_{33'}\overline{YH}}\left(\frac{Q-1}{Q + \frac{\overline{Y}}{K_{33'}\overline{YH}}}\right)^2 e^{-(\tau/\tau_{33'})}\right] \qquad (10)$$

One notices that the amplitudes Ξ are identical in both envisaged situations because $K_{13}/\overline{H} = \overline{Y}/(K_{33'}\overline{YH})$. In contrast, the chemical relaxation time that is observed in FCS is τ_{13} in the first case whereas it is $\tau_{33'}$ in the second.

D.2. Results. The preceding considerations were significant to measure rate constants by FCS. In fact, $\tau_{33'}$ could be typically lower than the time resolution of the autocorrelator at large enough concentrations in buffer. Then, no kinetic information could be extracted from $G(\tau)$. Therefore, we generally conducted the kinetic experiments in the absence of buffer. In particular, all the solutions were degazed before FCS measurement to avoid any possible interference with the acidic and basic species arising from dissolution of carbon dioxide.

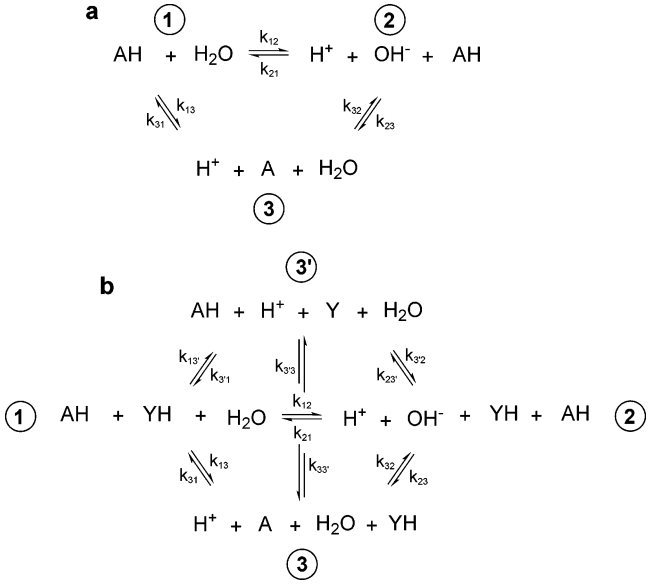

Figure 7. Reactions involved in the mechanism of dissociation/recombination of an acid−base couple, $\mathcal{AH}/\mathcal{A}$, in aqueous solution in the absence (a) or in the presence (b) of another acid−base couple, $\mathcal{YH}/\mathcal{Y}$.

We first prepared degazed unbuffered solutions of **4-PYMPO**, **4-PYMPO−NH$_2$**, and **4-PYMPOM** at a pH around their pK_a. Under such conditions, we extracted the pH from the fluorescence emission spectrum of each pH indicator by using a ratiometric approach relying on emission.[36,37] We also used under argon pH indicator sticks (precision: ±0.25 pH unit) or the indications of a pH meter when the latter were reliable. All indications were coherent with a precision that we estimate at 0.2 pH unit.

Figures 5b and 6c,d display typical experimental FCS autocorrelation curves for degazed solutions of **4-PYMPO**, **4-PYMPO−NH$_2$**, and **4-PYMPOM** at a pH around their pK_a in the absence of buffer. In relation to any chemical contribution to the correlation function, one is mainly concerned with the $G(0)$ value as well as with a possible new threshold manifesting itself in the correlation function.

For **4-PYMPO**, Figure 5b clearly evidences both features. At a similar nominal concentration of the solutions, $G(0)$ is much larger at pH = 4.6 (Figure 5b) than at pH = 2 (Figure 5a). Moreover, one notices two thresholds in the correlation function that is displayed in Figure 5b. The threshold associated with diffusion was already present in Figure 5a. In addition, there is another threshold at shorter times. To clear the origin of this second threshold, we first checked that it was not associated with the formation of the triplet state by recording FCS autocorrelation curves at different laser powers. They were essentially identical except for alterations of the signal-to-noise ratio. We also recorded the FCS autocorrelation curves from solutions of **4-PYMPO** at the same pH but in the presence of 100 mM buffer. In contrast to the experiment performed in the absence of buffer, the autocorrelation curve was essentially similar to the one recorded at pH = 2. This result was anticipated from eq 10 because $\tau_{33'}$ would be typically in the nanosecond range under such conditions. Therefore, we concluded that the second threshold displayed in Figure 5b was associated with the contribution of the reactive channel 13 to the autocorrelation function. Using $d = 370 \pm 30$ μm^2 s^{-1} and p$K_a = 4.3$,[37] we obtained the fit with eq 9 yielding $\overline{N}/V = 75 \pm 10$ nM, pH = 4.70 ± 0.05, and $\tau_{13} = 0.9 \pm 0.1$ μs. The extracted values of $\overline{N}/V$ and of pH are in line with the nominal concentration that was used during the experiment and the independent pH measurement. From pH and τ_{13}, we then derived $k_{13} = 8 \pm 1 \times 10^5$ s^{-1} and $k_{31} = 1.2 \pm 0.1 \times 10^{10}$ M^{-1} s^{-1}. k_{31} is close to the diffusion limit and is in line with the values reported for the comparable pyridine and imidazole.[42,43]

For **4-PYMPO−NH$_2$** and **4-PYMPOM**, the chemical signature is not as apparent as that for **4-PYMPO** in the autocorrelation curve at pH ≈ pK_a. In particular, only one threshold is visible in Figure 6c,d that were, respectively, recorded at pH = 6.1 and 6.0. Nevertheless, $G(0)$ clearly exceeds the corresponding value at a pH much lower than its pK_a for comparable nominal concentrations, and the previous observation suggests that chemical exchange is involved in the shape of the autocorrelation curves. Under such conditions, the possibility of access to the rate constants k_{13} and k_{31} depends on the relative values of τ_{13} and τ_D. As suggested by Figure 1b, the rate constants cannot be extracted anymore if $\tau_{13} \gg \tau_D$. We consequently attempted to fit the data shown in Figure 6c,d either with eq 4 (diffusion only) or with eq 9 (diffusion and chemical reaction). In fact, the fits with eq 4 reveal a systematic error that is not apparent when eq 9 is used. In the case of **4-PYMPO−NH$_2$**, we thus used $d = 470 \pm 30$ μm^2 s^{-1} and p$K_a = 5.7$[36,37] to extract from the fit with eq 9 $\overline{N}/V = 70 \pm 10$ nM, pH = 6.0 ± 0.1, $\tau_{13} = 25 \pm 1$ μs, $k_{13} = 3 \pm 1 \times 10^4$ s^{-1}, and $k_{31} = 1.3 \pm 0.2 \times 10^{10}$ M^{-1} s^{-1}. For **4-PYMPOM**, we correspondingly obtained with $d = 440 \pm 30$ μm^2 s^{-1} and p$K_a = 5.7$[37] $\overline{N}/V = 20 \pm 5$ nM, pH = 5.9 ± 0.1, $\tau_{13} = 20 \pm 1$ μs, $k_{13} = 3 \pm 1 \times 10^4$ s^{-1}, and $k_{31} = 1.5 \pm 0.2 \times 10^{10}$ M^{-1} s^{-1}. $\overline{N}/V$ and pH agree with the expectation from the nominal concentration and with the independent pH measurement. Noticeably, the k_{31} values observed for **4-PYMPO−NH$_2$** and **4-PYMPOM** are again close to the diffusion limit.[42,43] These results suggest that the presence of one ortho amino, or two ortho methyl substituents, does not significantly affect the rate of reaction of the nitrogen lone pair of the pyridine ring with the proton.

pH Measurements by FCS. A. General Case. As indicated in the Theoretical Analysis section, the issues of measuring rate constants or reactant concentrations by FCS are closely related. Thus, the autocorrelation curves displayed in Figures 5b and 6c,d can be used to illustrate how FCS should yield pH in a general case.

Provided that one considers that the pK_a and the brightness of both acidic and basic states of the pH indicator are known in the investigated medium, the analysis of the amplitude of the autocorrelation function would provide pH after fitting with eq 3. Indeed, the pH extracted from the fits in Figures 5b and 6c,d are in fair agreement with the pH value measured by other methods. Independently, pH can also be extracted from the time dependence of the autocorrelation function if one knows the pK_a and k_{31} for the fluorescent pH indicator. Ultimately, both methods can be applied to evaluate the coherence of the results if all the relevant information about the fluorescence pH indicator is available and reliable.

B. Example of Calibration-Free pH Measurement. B.1. Evaluation of the Constraints on the Fluorescent pH Indicator. The "calibration-free approach" requires that (i) the protonation of the fluorescent pH indicator is controlled by

diffusion and (ii) it is possible to find experimental conditions (excitation wavelength, optical filters, etc.) such that the fluorescence emission from one state, acidic or basic, may be neglected with regards to the other under the same conditions.

The preceding measurements in water showed that the protonation of the pyridine basic site is indeed limited by diffusion for **4-PYMPO**, **4-PYMPO−NH$_2$**, and **4-PYMPOM**. In an unknown medium, questions still arise as to whether (i) diffusion is still the limiting process for protonation and (ii) D and a in eq 6 are medium-dependent (d can be directly evaluated from the diffusion contribution in the autocorrelation function). In relation to the former question, one has to be concerned with the energy barrier associated with the solvent reorganization occurring during protonation.[48] Water is a strongly polar solvent that is anticipated to promote among the largest corresponding energy barriers. Even in water, the measured k_{31} value does not reveal the presence of such a barrier. Other conditions should be typically less polar, and the barrier should not manifest either. In relation to the latter, two main issues have to be addressed. We first notice that a should not strongly depend on the ionic strength[39] because the present probes do not involve highly charged species. In contrast, water develops a particular relation to the proton. This feature may determine too large values of D and a with regard to predictions that would only rely on the proton diameter and on the solvent viscosity.[1,39] In fact, we estimate that the k_{31} value should not depart from 1×10^{10} to 2×10^{10} M^{-1} s^{-1} by a factor exceeding a few units for most situations encountered in common liquids. In view of the logarithmic dependence of pH on proton concentration, the corresponding incertitude on k_{31} should introduce at most an error of a few tenths on the extracted pH.

We investigated the photophysical features and the significance of solvatochromism on the absorption and emission properties of **4-PYMPO** and **4-PYMPO−NH$_2$** in a preceding report.[37] **4-PYMPOM** is expected to exhibit a behavior similar to that of **4-PYMPO** because the methyl substituents generally only slightly alter photophysical properties. First, the absorption and the fluorescence emission occur at larger wavelengths for the acidic state than for the basic state (see Figure 4). In the present series, we also showed the following: (i) The maximum of single-photon absorption is not sensitive to solvent polarity for the neutral basic states, whereas it slightly drops when solvent polarity is increased for the charged acidic state. In relation to two-photon absorption, we expect a similar trend because two-photon absorption spectra generally satisfactorily compare with the one-photon absorption spectra after dividing the wavelength by a factor of 2 for unsymmetrical compounds.[49,50] (ii) The maximum of emission after single-photon absorption increases with the solvent polarity for the basic state, whereas it is not significantly sensitive to solvent polarity for the acidic state. Thus, the photophysical features brought us to conclude that one could easily find a large enough excitation wavelength to considerably and selectively excite the acidic state of the present fluorescent indicators ($\mathcal{Q}_{\mathcal{M}} \gg \mathcal{Q}_{\mathcal{A}}$), whatever the medium considered.

In principle, the three present fluorescent pH probes were appropriate to evaluate the calibration-free approach. Upon consideration of the similarity of their photophysical properties, the final choice would essentially rely on the proton concentration $\overline{H}$ to be measured because one ideally looks for a fluorescent pH indicator such that $\overline{H} = 10^{-pK_a}$. We retained **4-PYMPOM** for the following series of experiments.

B.2. Results. To evaluate the calibration-free approach that was evoked above, we conceived model experiments. We considered a solvent containing various amounts of a strong acid (triflic acid/CF_3SO_3H), and we aimed at using FCS and **4-PYMPOM** to determine the unknown concentrations in the proton. In parallel, we measured the protonation constant of **4-PYMPOM** and calibrated a pH meter used to monitor the proton activity in the corresponding solvent. This allowed us to evaluate the validity of the FCS results by directly measuring pH either from a ratiometric approach relying on fluorescence emission or from the pH meter indication after an appropriate calibration.

We chose to work in a mixture of water and acetonitrile to perform this series of experiments. In fact, this system remains simple for model experiments, but the corresponding solvent organization is rather controversial.[51] In particular, one cannot reasonably assume that the **4-PYMPOM** photophysical (quantum yields of fluorescence, lifetimes, etc.) and acidobasic (pK_a) properties should be identical in water and in the acetonitrile/water mixture. In such a context, **4-PYMPOM** should be a priori useless as a fluorescent pH indicator with a classical approach requiring the preliminary knowledge of the items (iii)−(iv) evoked in the Introduction.

The acetonitrile/water ratio was optimized (i) by reducing the water content to essentially suppress the protonation of the basic state of **4-PYMPOM** that occurs during the lifetime of its excited state[37] and (ii) by maintaining an as large as possible water content to facilitate the calibration of the pH meter using a glass electrode conditioned in water. We retained 60:40 (v/v) acetonitrile/water as a solvent.

Figure 8a displays a typical FCS autocorrelation curve that was recorded from a solution of **4-PYMPOM** in 60:40 (v/v) acetonitrile/water solution at an "unknown" proton concentration. In line with the calibration-free approach, the experimental data were fitted with eq 9 by taking $k_{31} = 2.0 \times 10^{10}$ M^{-1} s^{-1} as the only fixed parameter. We found $\overline{N}/V = 40 \pm 10$ nM, $\tau_D = 30$ μs, $pK_a = 5.1$, and $\overline{H} = 10 \pm 1$ μM.[52]

The extracted value of $\overline{N}/V$ was in line with the nominal **4-PYMPOM** concentration. τ_D reasonably compared with the diffusion time that was observed in the presence of an excess

(48) For an illustration of the role of solvent reorganization during a chemical reaction, see, for instance: Laage, D.; Thompson, W. H.; Blanchard-Desce, M.; Hynes, J. T. *J. Phys. Chem. A* **2003**, *107*, 6032−6046.
(49) Cogné-Laage, E.; Allemand, J.-F.; Ruel, O.; Baudin, J.-B.; Croquette, V.; Blanchard-Desce, M.; Jullien, L. *Chem.−Eur. J.* **2004**, *10*, 1445−1455.
(50) Xu, C.; Webb, W. W. *J. Opt. Soc. Am. B* **1996**, *13*, 481−491.
(51) Catalán, J.; Díaz, C.; García-Blanco, F. *Org. Biomol. Chem.* **2003**, *1*, 575−580.
(52) We performed preliminary simulations to evaluate the reliability of the parameter values that can be extracted from FCS autocorrelation curves by using eq 9. We used eq 3 to generate FCS autocorrelation curves $G_f(\tau)$ with $\overline{N} = 1$, $\omega = 10$, $\overline{H} = K$, and $Q = \infty$ for different $k\tau_D$ values. Then, we introduced some noise in the calculated autocorrelation functions to simulate "experimental" autocorrelation functions $G_e(\tau)$ by adopting the typical noise level that was observed during our present FCS measurements ($-0.1 < [G_e(\tau) - G_f(\tau)]/G_f(\tau) < 0.1$). We finally used eq 9 to fit the simulated experimental data in the 10^{-3}−10^3 range for (τ/τ_D) by using $k\tau_D$, $\overline{N}$, and ($K/\overline{H}$) as floating parameters. The results are given in Supporting Information Table 2S and Figure 4S. The values of the extracted parameters never deviate from the expected ones by more than 40% as long as $100 > k\tau_D > 0.1$. They are at the most satisfactory for $k\tau_D = 1-10$ where the threshold associated to the chemical reaction is at the most visible in the FCS autocorrelation curve.

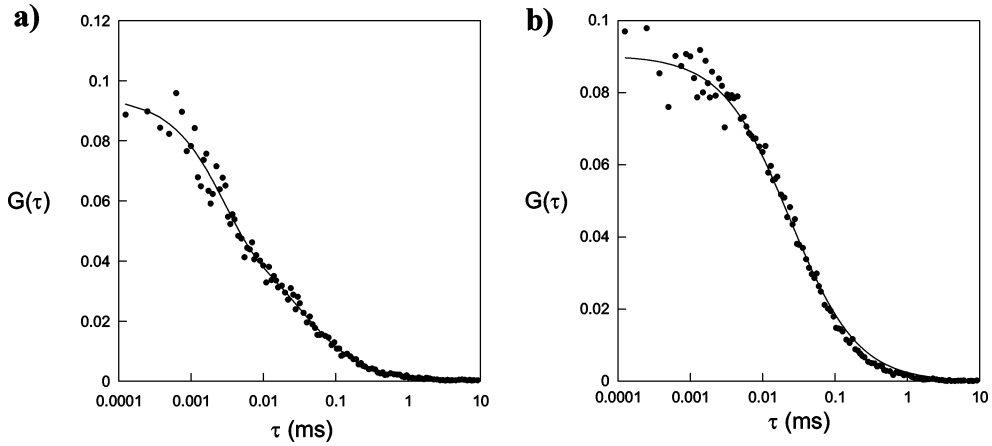

Figure 8. FCS autocorrelation curves recorded at 293 K from solutions of **4-PYMPOM** in 60:40 (v/v) acetonitrile/water solution ($\lambda_{exc}^{(2)} = 800$ nm). (a) At "unknown" proton concentration ($\lambda_{exc}^{(2)} = 800$ nm) ($\overline{H} = 6$ μM). Using $k_{31} = 2 \times 10^{10}$ M^{-1} s^{-1}, the fit with eq 3 yields $\overline{N}/V = 40 \pm 10$ nM, $\tau_D = 30$ μs, pK_a = 5.1 and $\overline{H} \approx 10 \pm 1$ μM. (b) Large excess of proton ($\overline{H} \approx 4$ mM). The fit according to eq 4 yields $\overline{N}/V = 20 \pm 5$ nM and $d = 690 \pm 30$ μm^2 s^{-1}.

of acid. In fact, we expected $\tau_D \approx 25$ μs from the 690 ± 30 μm^2 s^{-1} value of the **4-PYMPOM** diffusion coefficient that was extracted from fitting the data shown in Figure 8b with eq 4. Using the value of the **4-PYMPOM** diffusion coefficient obtained in water as a reference and considering that the diffusion coefficient is inversely proportional to medium viscosity η, we should deduce $\eta = 0.9$ Pa s for the viscosity of the unknown medium (0.6 Pa s from the reference experiment illustrated in Figure 8b). These values are in reasonable agreement with available literature data that give 0.8 Pa s for the viscosity of 60:40 (v/v) acetonitrile/water.[53]

The pK_a was independently extracted from analyzing the evolution of **4-PYMPOM** fluorescence emission in 60:40 (v/v) acetonitrile/water as a function of the concentration in triflic acid. As shown in Figure 9a, the addition of a proton promotes the drop in emission from the **4-PYMPOM** basic state and the increase of the red shifted band associated to the **4-PYMPOM** acidic state. Thus, we found pK_a = 5.3 ± 0.1. This value satisfactorily compares with the value that was directly extracted from the FCS data.

To evaluate the unknown concentration in the proton independently of the FCS measurement, we relied on two different tools. We first used **4-PYMPOM** as a fluorescent pH indicator to extract the proton concentration from the ratiometric analysis in emission, displayed in Figure 9b. We also used the indication pH′ of the glass electrode of a pH meter that was preliminarily calibrated by recording the indication from standard solutions that contained known concentrations, $\overline{H}$, in the proton. We obtained $\overline{H} = 6$ μM under the conditions used to record the FCS autocorrelation curve of Figure 8a. The comparison against the FCS result is again favorable.

Eventually, we directly measured the rate constant k_{31} to evaluate the value that was taken a priori. We analyzed the dependence of $1/\tau_{13}$ on $(1 + (1/\Xi))$ in a series of experiments at different proton concentrations in 60:40 (v/v) acetonitrile/water.

$$\frac{1}{\tau_{13}} = k_{13}\left(1 + \frac{1}{\Xi}\right) \qquad (11)$$

The results are displayed in Figure 9c. Indeed, we found that τ_{13} is linearly dependent on $1 + (1/\Xi)$. In addition, we extracted $k_{31} = 3.2 \pm (0.2 \times 10^{10})$ M^{-1} s^{-1} from the slope of the linear fit displayed in Figure 9c. Such a larger value than the one found in water is in line with the low viscosity of the 60:40 (v/v) acetonitrile/water mixture. By correcting the value measured in water by the relative viscosity of the present solvent to the one of water (0.6), we expected $k_{31} \approx 2.5 \times 10^{10}$ M^{-1} s^{-1}.

In relation to the calibration-free approach, the directly measured k_{31} value is close to the one that we used a priori. To evaluate the significance of the error in using 2×10^{10} M^{-1} s^{-1} instead of $3.2 \pm (0.2 \times 10^{10})$ M^{-1} s^{-1} for the k_{31} value, we again fitted with eq 6 the data displayed in Figure 8a. As expected, we did not notice any considerable change with regards to the extracted values of $\overline{H}$ and pK_a: 6 μM and 5.2, respectively, were found.

C. Discussion. The preceding experiments confirm that FCS provides a powerful approach to measure reactant concentrations. In the case of the proton, we showed that a proper design of the fluorescent pH indicator makes it possible to measure pH between 4 and 6 with FCS after two-photon excitation. The lower limit is actually set by the present time resolution of the autocorrelator. In principle, pH indicators with pK_a around 9 would similarly open the way to pH measurements between 8 and 10. Indeed, the rate constants for reaction between the acidic states of fluorescent pH indicators and the hydroxide ion are generally limited by diffusion[42] so as to lead to results similar to the present ones after symmetry around pH = 7. In contrast, it seems difficult to cover the 6−8 pH range when FCS after two-photon excitation is used. In fact, the low concentration in the proton or in hydroxide yields $\tau_\chi > \tau_D$ under such conditions. From this point of view, FCS after one-photon excitation seems more advantageous to continuously cover the 4−10 pH range[19] because appropriate optical setup allows $\tau_\chi < \tau_D$ in the whole range of pHs.

As far as the present FCS calibration-free titration approach is concerned, we showed that it is indeed possible to extract pH without preliminary calibration from a FCS autocorrelation curve after a proper design of the fluorescent pH probe. Although rather limited in most cases, the error on the reactant concentration should mainly originate from the uncertainty on

(53) The data are provided by the Waters Company. HPLC Troubleshooting, Neue, U. D., Waters Corporation, www.waters.com.

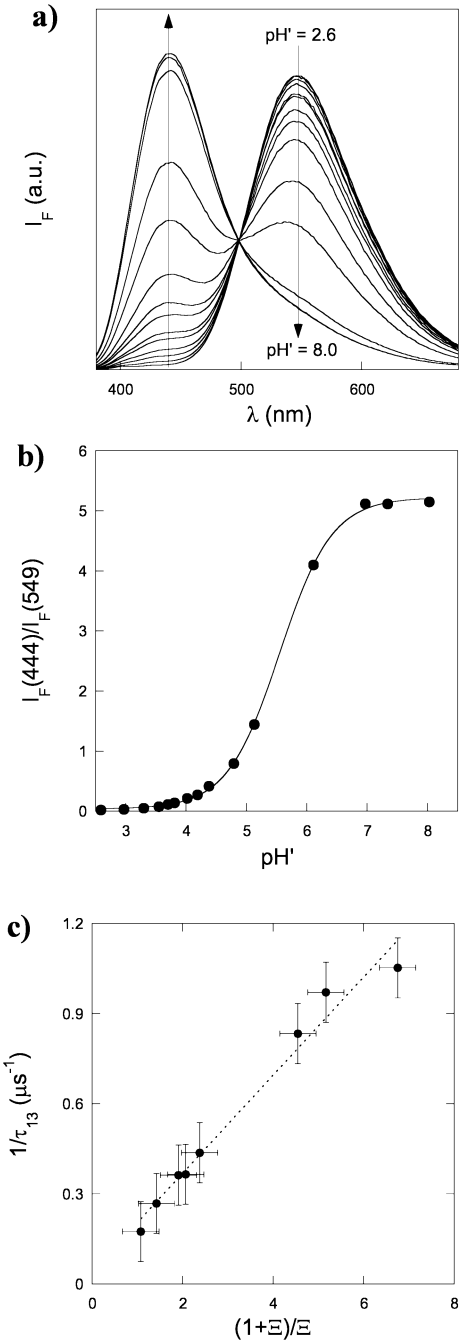

Figure 9. (a) Dependence on pH′ of the emission spectra of **4-PYMPOM** after one-photon excitation (from acidic to basic: pH′ = 2.6, 3.0, 3.3, 3.5, 3.7, 3.8, 4.0, 4.2, 4.4, 4.8, 5.1, 6.1, 7.0, 8.0). (b) Evolution on pH′ of the ratio of the fluorescence emissions at 444 and at 549 nm after one-photon excitation. Experimental data markers: fit = line. $\lambda_{exc}^{(1)}$ = 355 nm and [**4-PYMPOM**] = 5 μM. (c) Dependence of $1/\tau_{13}$ on $1/\Xi$. τ_{13} and Ξ were extracted from a series of FCS experiments at different proton concentrations. Solvent: acetonitrile/water 60:40 (v/v), T = 293 K. See text and Experimental Section.

the value of the rate constant of association of the reactant with the fluorescent probe. A satisfactory order of magnitude of this can be evaluated with eq 6 by using parameter values extracted from the autocorrelation function (*d* and *D* from the diffusion contribution that yields the local viscosity) and from the structures of the probe and of the reactant (*a* and the geometrical factors involved in *d* and *D*). Here, it is worth it to emphasize that the classical approaches for titrations with fluorescent probes rely on values of parameters (association constants and photophysical features) that cannot be easily predicted in an unknown medium on the basis of the structures of the reactant and on the probe only.

Making FCS a superior tool to measure reactant concentrations requires us to rely on the kinetic information of the FCS autocorrelation function. Beyond the photophysical and the thermodynamic aspects that may already be demanding, a proper molecular design of the kinetic properties of the fluorescent probes is a crucial issue here. Ideally, the relaxation pathways after fluctuations from equilibrium should be known and controlled, even when dealing with unknown media. In fact, it is the capability to reduce the interference of buffering species that will probably determine the impact of FCS for measuring reactant concentrations. If the information related to the buffer is lacking (like in a biological cell for instance), the buffer will "only" complicate the analysis of the kinetic content of the autocorrelation curve in the best case. Yet, it can even forbid any concentration measurement if it dominates the relaxation with a chemical relaxation time lower than the temporal resolution of the autocorrelator.

From the previous point of view, reliable pH measurement under any situation will be design demanding. In the present work, we envisaged the reduction of the rate constants involving the 33′ exchange without strongly altering k_{31} by playing with the steric hindrance around the basic site of $\mathcal{A}$. We did succeed in keeping k_{31} at the largest for the three investigated fluorescent pH indicators. In contrast, we failed to decrease enough $k_{33'}$ to measure pH by FCS in 100 mM buffered solutions with any present pH probe (if one assumes that one of the reactions in the 33′ channel is limited by diffusion,[42] the crossing between both regions governing the relaxation of the fluctuations, τ_{13} or $\tau_{33'}$, occurs as low as 10^{-4} M for a buffer with p$K_a(\mathcal{HA}/\mathcal{A}) \approx$ 5). With such nonoptimized pH probes, we had thus to totally control the composition and the reactivity of the medium in a purpose of validation of the present FCS approach to measure proton concentration: We consequently adopted rather severe experimental conditions (degazing of the solutions to avoid interference with any buffer arising from dissolution of carbon dioxide, absence of added buffer, etc.). To face the measurement of proton concentration in an unknown media, one would ideally design an improved fluorescent pH probe with a proton exchange that would occur in the 10 μs range via the 13 reactive channel without any interference of the 33′ reactive channel. At that point, it is interesting to notice that it was possible to measure rate constants for proton exchange in the green fluorescent protein (GFP) in heavily buffered media.[19,25−27] This observation suggests that coupling fluorescent pH indicators to acid−base of appropriate pK_a by a specific channel for the proton could provide attractive opportunities.

4. Conclusion

Fluorescence correlation spectroscopy clearly opens new roads for using specific fluorescent probes in the analysis of local reactant concentrations. Under many encountered situations, data treatment only involves simple analytical expressions that are derived after appropriate approximations. Under the less favorable circumstances, to extract an unknown reactant concentration from FCS data requires the same photophysical and thermodynamic information as that in a ratiometric approach. Nevertheless, the kinetic information contained in the FCS

observable may provide a distinct advantage to evaluate the coherence of the results and to improve the selectivity of the analysis. In the best cases, it is even possible to evaluate reactant concentrations in the absence of any preliminary calibration.

This report also emphasizes that the development of FCS as a powerful analytical tool will strongly depend on the availability of carefully tailored fluorescent indicators. Thermodynamic and photophysical constraints have first to be taken into account. Such criteria are rather classical to design specific fluorescent probes. Nevertheless, here probe brightness deserves special attention in relation to the submicromolar requirements of FCS, in particular, when multiphoton excitation is used. More unusual are the kinetic constraints to avoid interferences with buffering species that can alter or even cancel the relevant information contained in the FCS observable. In the present account, we engineered a series of fluorescent probes to illustrate the exciting opportunities provided by FCS after two-photon excitation to measure pH in a given range. Yet, performing reliable pH measurement in the absence of any information on buffering species is still challenging and will require further refinement in the molecular design of synthetic fluorescent probes.

5. Experimental Section

Chemicals. The syntheses of **4-PYMPO**, **4-PYMPO−NH$_2$**, and **4-PYMPOM** have already been reported elsewhere.[37] The analytical grade chemicals purchased from Aldrich were used without further purification. The 18 MΩ cm water was obtained from a Millipore setup. Acetonitrile was of spectroscopic grade.

Preparation of the Solutions. Stock solutions (50 μM) of the fluorescent pH indicators were prepared in 10^{-2} M triflic acid. These stock solutions were subsequently diluted to 100 nM in fluorescent pH indicators, either in 10^{-2} M triflic acid or in 10^{-2} M sodium hydroxide (measurement of diffusion coefficients at pH = 2 or pH = 12) or in water with pH adjustment with diluted solutions of triflic acid or sodium hydroxide (measurements at pH ≈ pK_a).

For the experiments performed in the presence of buffer, we used a Britton-Robinson buffer at 0.1 mol L^{-1} prepared according to ref 45.

Degazing was obtained by applying several freeze-thaw cycles to the solutions under a 1 mmHg vacuum. After the last cycle, the solution was settled under argon. It was eventually poured into the cell displayed in Supporting Information Figure 2S that was sealed under argon.

pH and pK_a Measurements. pH measurements were performed on a Standard pH meter PHM210-Radiometer Analytical that was calibrated with buffers at pH 4 and 7. For the measurements in the neutral solutions in the absence of any supporting salt (5 ≤ pH ≤ 7), we relied on indicator sticks (precision: ±0.25 pH unit).

To evaluate the concentration in the proton in a 60:40 (v:v) acetonitrile/water solution, we relied on the indication pH′ of the glass electrode of a pH meter that was preliminarily calibrated by recording the indication from standard solutions that contained known concentrations, $\bar{H}$, in the proton. Then, the experimental data were fitted according to a linear law. We obtained $-\log \bar{H}(M) = 8.09 \times 10^{-2} + 1.075$ pH′.

The evolutions of **4-PYMPOM** fluorescence in acetonitrile/water as a function of the concentration in the proton was analyzed with the SPECFIT/32TM Global Analysis System (Version 3.0 for 32-bit Windows systems) to extract the pK_a of the **4-PYMPOM** ground state.[54]

Spectroscopic Measurements. During the recording of the emission spectra, the temperature was regulated at 0.1 °C and was directly measured within the cuvettes.

Corrected fluorescence spectra were obtained from a Photon Technology International LPS 220 spectrofluorimeter (Photon Technology International, Monmouth Junction, NJ). Solutions for fluorescence measurements were adjusted to concentrations such that the absorption was below 0.15 at the excitation wavelength. The overall fluorescence quantum yields Φ_F were calculated from the relation in eq 12 where

$$\Phi_F = \Phi_{ref} \frac{A_{ref}(\lambda_{exc})}{A(\lambda_{exc})} \frac{S}{S_{ref}} \left(\frac{n}{n_{ref}}\right)^2 \quad (12)$$

the subscript ref stands for standard samples. $A(\lambda_{exc})$ is the absorbance at the excitation wavelength, S is the integrated emission spectrum, and n is the refractive index for the solvent. The uncertainty in the experimental value of Φ_F was estimated to be ±10%. The standard fluorophore for the quantum yield measurements was quinine sulfate in 0.1 M H_2SO_4 with $\Phi_{ref} = 0.50$.[55]

The two-photon excitation spectra were recorded with a home-built setup[49] using the reported excitation spectrum of fluorescein for calibration.[50]

FCS Measurements. The two-photon excitation FCS setup displayed in Supporting Information Figure 1S consists of a laser source, a home-built microscope, and two avalanche photodiodes (APD).[56] The laser source is a mode-locked Ti/Sapphire laser (Mira 900, Coherent, Auburn, CA) pumped by a solid-state laser at 532 nm (Verdi, Coherent). Pumped at 5 W, the Ti/Sapphire laser generates 150 fs pulses at a 76 MHz repetition rate with about 700 mW average power output at 800 nm. The power is adjusted by means of neutral filters. The laser beam is expanded 3 times at the entrance of the microscope to reach a diameter of approximately 7 mm to fill up the back entrance of the employed objective. After the beam expander, the light is passed through a dichroic mirror and focused into the sample with a 60 times water-immersion objective (NA = 1.2, UPlanApo, Olympus). The fluorescence is collected through the same objective, reflected by the dichroic mirror, and filtered through short pass filters to absorb any possible diffused excitation infrared light. The light is then separated by a cube beam splitter with a 1:1 ratio and focused on the 200 μm^2 working surfaces of two APDs (SPCM-AQR-14, Perkin-Elmer, Vaudreuil, Canada). At the concentrations used throughout this paper, the typical signal on each APD was about 20 kHz during the experiments devoted to the measurement of the diffusion coefficients, whereas we typically obtained 6 kHz during the experiments where the chemical reaction was involved. The signal outputs of the APD modules (TTL pulses) are acquired by a digital autocorrelator module (ALV-6000, ALV, Langen, Germany) which computes online the cross-correlation function of the fluorescence fluctuations. The data are then stored in the computer and analyzed by a home-written routine which allows us to (i) select and average chosen successive acquisitions, (ii) make a least-squares fit for both single- and two-component cross-correlation functions with diffusion in two or three dimensions, and (iii) calculate the associated standard deviations.

The focused beam was assumed to adopt a 3D-Gaussian excitation profile characterized by $I = I_0 \exp[-(2(x^2 + y^2)/\omega_{xy}^2) - (2z^2/\omega_z^2)]$. It was calibrated before each measurement by using the diffusion of fluorescein in water at pH = 10 as a standard.[14] We typically obtained $\omega_{xy} \approx 0.4$ μm and $\omega_z/\omega_{xy} \approx 10$.

We investigated the dependence of the fluorescence emission as a function of the excitation power for all the compounds studied, and we chose the power to remain in the region of power-squared dependence (as a rule, the power before the entrance of the beam

(54) Gampp, H.; Maeder, M.; Meyer, C. J.; Zuberbühler, A. D. *Talanta* **1985**, *32*, 95−101. Gampp, H.; Maeder, M.; Meyer, C. J.; Zuberbühler, A. D. *Talanta* **1985**, *32*, 257−264. Gampp, H.; Maeder, M.; Meyer, C. J.; Zuberbühler, A. D. *Talanta* **1985**, *32*, 1133−1139. Gampp, H.; Maeder, M.; Meyer, C. J.; Zuberbühler, A. D. *Talanta* **1986**, *33*, 943−951.

(55) Demas, J. N.; Crosby, G. A. *J. Phys. Chem.* **1971**, *75*, 991−1024.

(56) Gosse, C.; Boutorine, A.; Aujard, I.; Chami, M.; Kononov, A.; Cogné-Laage, E.; Allemand, J.-F.; Li, J.; Jullien, L. *J. Phys. Chem. B* **2004**, *108*, 6485−6497.

expander was set to less than 60 mW). With those experimental conditions, no contribution of the triplet state to the experimental FCS curves was observed either.

A typical experiment consisted of a few hundreds of acquisitions of 2−5 s each, depending on the overall brightness, thus leading to a typical 30 min−2 h acquisition time.

Acknowledgment. This paper is dedicated to the memory of Professor André Rassat.

Supporting Information Available: Computation of the auto- and cross-correlation functions that are relevant to the present work. Experimental FCS setup (Figure 1S), sample-containing cell that was used during the present FCS experiments (Figure 2S), chemical process involving the smallest number of interconverting states that can be observed by FCS (Figure 3S), evaluation of the reliability of the parameter values that can be extracted from FCS autocorrelation curves by using eq 9 (Figure 4S), derivation of the intrinsic relaxation times τ_{ij} associated with the six chemical reactions displayed in Figure 7b (Table 1S), and evaluation of the reliability of the parameter values that can be extracted from FCS autocorrelation curves by using eq 9 (Table 2S). This material is available free of charge via the Internet at http://pubs.acs.org.

JA053909W